




## Differentially spliced mitochondrial CYP419A1 contributes to ethiprole resistance in *Nilaparvata lugens*

B. Zeng<sup>a,1</sup>, A.J. Hayward<sup>a,1</sup>, A. Pym<sup>a</sup>, A. Duarte<sup>a</sup>, W.T. Garrood<sup>b,2</sup>, S-F Wu<sup>c,d</sup>, C-F Gao<sup>c,d</sup>, C. Zimmer<sup>a,3</sup>, M. Mallott<sup>a</sup>, T.G.E. Davies<sup>b</sup>, R. Nauen<sup>e</sup>, C. Bass<sup>a,\*</sup>, B.J. Troczka<sup>a,\*</sup> 

<sup>a</sup> Centre for Ecology and Conservation, Biosciences, University of Exeter, Penryn Campus, Penryn, Cornwall, UK

<sup>b</sup> Insect Molecular Genomics Group, Protecting Crops and the Environment, Rothamsted Research, Harpenden, UK

<sup>c</sup> College of Plant Protection, Nanjing Agricultural University, Nanjing, People's Republic of China

<sup>d</sup> State & Local Joint Engineering Research Center of Green Pesticide Invention and Application, Jiangsu, People's Republic of China

<sup>e</sup> Bayer AG, Bayer CropScience Division R&D, Monheim am Rhein, 40789, Germany

### ABSTRACT

The brown planthopper *Nilaparvata lugens* is one of the most economically important pests of cultivated rice in Southeast Asia. Extensive use of insecticide treatments, such as imidacloprid, fipronil and ethiprole, has resulted in the emergence of multiple resistant strains of *N. lugens*. Previous investigation of the mechanisms of resistance to imidacloprid and ethiprole demonstrated that overexpression and qualitative changes in the cytochrome P450 gene *CYP6E1* lead to enhanced metabolic detoxification of these compounds. Here, we present the identification of a secondary mechanism enhancing ethiprole resistance mediated by differential splicing and overexpression of CYP419A1, a planthopper-specific, mitochondrial P450 gene. Although metabolic resistance to insecticides is usually mediated by overexpression of P450 genes belonging to either CYP 3 or 4 clades, we validate the protective effect of over-expression of CYP419A1, *in vivo*, using transgenic *Drosophila melanogaster*. Additionally, we report some unusual features of both the CYP419A1 gene locus and protein, which include, altered splicing associated with resistance, a non-canonical heme-binding motif and an extreme 5' end extension of the open reading frame. These results provide insight into the molecular mechanisms underpinning resistance to insecticides and have applied implications for the control of a highly damaging crop pest.

### 1. Introduction

The brown planthopper (BPH) *Nilaparvata lugens* (Hemiptera: Delphacidae) is one of the most economically important pests of cultivated rice in Southeast Asia. It causes damage both through direct phloem feeding and transmission of plant viruses. Severe outbreaks result in so-called “hopper burns” and can cause an estimated 80% loss of total planted crop (Health et al., 2023). Synthetic insecticides are used as the primary method of control with the consequent result of strong selection for resistance to a diverse range of compounds, with high levels of resistance reported for imidacloprid, pymetrozine, buprofezin, fipronil and ethiprole, to name a few (Wu et al., 2018). Ethiprole is a phenyl-pyrazole insecticide acting as a non-competitive inhibitor of GABA-gated chloride channels (Rdl) (Cole et al., 1993). It is a broad-spectrum insecticide targeting chewing and sucking insects in a wide range of crops, including cotton, corn and rice (Caboni et al., 2003)

and exhibits good insect specificity and a low mammalian toxicity (Ratra and Casida, 2001). According to the Insecticide Resistance Action Committee (IRAC) ethiprole, together with its close relative fipronil, belongs to mode of action group 2B (GABA channel blockers) (Nauen et al., 2019). Due to toxicity concerns with fipronil, ethiprole became the more popular compound of choice for control of BPH in Asia, which quickly resulted in emergence of resistance (Garrood et al., 2016). Investigation of the underlying molecular mechanisms of ethiprole resistance initially identified a point mutation resulting in the A301S substitution in the *Rdl* gene (Zhang et al., 2016). Garrood et al. identified two more strains from Thailand and India NI33 (named NLF2 here) and NI55 which carried the A301S mutation at a low frequency but were selected to fixation upon continuous exposure to ethiprole (Garrood et al., 2017). *In vitro* and *in vivo* analysis of A301S showed it contributed to, but could not fully explain, the highly resistant phenotype observed in both strains upon selection (Garrood et al., 2017). Subsequent

\* Corresponding author.

\*\* Corresponding author.

E-mail addresses: [c.bass@exeter.ac.uk](mailto:c.bass@exeter.ac.uk) (C. Bass), [b.troczka@exeter.ac.uk](mailto:b.troczka@exeter.ac.uk) (B.J. Troczka).

<sup>1</sup> Authors contributed equally.

<sup>2</sup> Present address: Wellcome Trust, 215 Euston Road, London, NW1 2BE.

<sup>3</sup> Present address: Syngenta Crop Protection, Werk Stein, Schaffhauserstrasse, Stein CH4332, Switzerland.

investigations identified the primary mechanism of ethiprole, as well as imidacloprid, resistance was mediated by gene duplication, over-expression and neofunctionalization of the cytochrome P450 gene, *CYP6ER1* (Zimmer et al., 2018; Duarte et al., 2022). A series of point mutations (T318S, P377del, A375del and A376G) in two substrate recognition sites (SRS) of one of the copies of the duplicated *CYP6ER1* gene resulted in improved imidacloprid detoxification, while a second set of point mutations, outside of the known SRS regions (T176K, S346A and V436I), were shown to improve ethiprole detoxification (Duarte et al., 2022). Moreover, *CYP6ER1* was also shown to metabolise other neonicotinoids as well as the butenolide flupyradifurone (Hamada et al., 2020).

Cytochrome P450s are a large superfamily of heme-containing enzymes which are ubiquitous across the entire tree of life. They are responsible for metabolising a myriad of both exogenous and endogenous substrates (Dermauw et al., 2020). P450s are phase I enzymes in xenobiotic detoxification pathways and often play a crucial role in the metabolism of synthetic insecticides and the emergence of resistance (Nauen et al., 2022). In insects, P450s belonging to the large and diverse CYP3 and CYP4 clans are most commonly involved in xenobiotic detoxification, for example the above-mentioned *CYP6ER1* belongs to the CYP3 clan (Nauen et al., 2022). In comparison, the mitochondrial clan usually consists of a small number of highly conserved genes, with most insect species possessing only a few members (Dermauw et al., 2020). In *Drosophila melanogaster*, and other insects, members of the mitochondrial clan (*CYP314A1*, *CYP302A1* and *CYP315A1*) are involved in the developmentally crucial ecdysteroidogenic pathway (Petryk et al., 2003; Warren et al., 2002; Jia et al., 2013). The name of the clan originally comes from the subcellular localisation, true mitochondrial P450s also require different redox partners, namely ferredoxin (Adx) or NADPH-dependent ferredoxin reductase (Guzov et al., 1998) (AdR). Although in insects few members of the mitochondrial clan have been shown to be exclusively expressed in the organelle and for most genes the association is based on phylogeny and *in silico* analysis alone (Dermauw et al., 2020).

In this manuscript, we describe an unusual secondary mechanism contributing to ethiprole resistance in a multiple insecticide resistant strain (NLF-2) of *N. lugens* mediated by overexpression of a truncated form of the mitochondrial P450, *CYP419A1*.

## 2. Methods

### 2.1. Chemicals

All standalone chemicals, technical grade (purity <99%) ethiprole, fipronil and imidacloprid used were purchased from Merck (Germany).

### 2.2. Insect strains

Details on the insect strains used in the study (NLS, NLF2, NLF2eth) have been described previously (Zimmer et al., 2018). Briefly NLS strain is a laboratory susceptible reference (ethiprole LC<sub>50</sub> 0.34 mg/L 0.24–0.44 95%CI), while NLF2 is a field collected strain originating from South Vietnam (ethiprole LC<sub>50</sub> 138.3 mg/L 90.82–198.3 95% CI), and NLF2eth is an ethiprole-selected laboratory variant of NLF2 with LC<sub>50</sub> > 5000 mg/L).

### 2.3. Nucleic acids extraction and reverse transcription

Total RNA was extracted from a pool of 5 (transgenic *D. melanogaster*) or 10 (*N. lugens*) adults using the Isolate II RNA mini kit (Meridian Bioscience, USA) following the manufacturer's protocol. The quality of RNA was verified using Nanodrop, Qubit™ Broad range RNA kit (ThermoFisher Scientific, USA), and agarose gel electrophoresis. One µg of total RNA was used for cDNA synthesis using the Maxima H Minus Reverse Transcriptase and random hexamers (qPCR) or Oligo(dT)<sub>15</sub> (RT-

PCR) (ThermoFisher Scientific, USA) following the manufacturer's protocol. Genomic DNA from *N. lugens* was extracted using the E.Z.N.A mollusc DNA kit (Omega Bio-Tek) following the manufacturer's protocol.

### 2.4. PCR and qPCR

All qPCR reactions (15 µl) contained, 7.5 µl of SYBR® Green Jump-Start™ Taq ReadyMix (Merck, Germany), 4 µl of cDNA or gDNA (5 ng) and 0.25 µM of each primer (Supplementary Table 1). Cycling conditions comprised: 3 min at 95 °C, followed by 40 cycles of 95 °C for 15s, 58 °C for 15s and 72 °C for 15s. A final melt-curve step was included post-PCR (ramping from 65 to 95 °C by 0.5 °C every 5s) to confirm the absence of any non-specific amplification. The efficiency of PCR for each primer pair was assessed using a serial dilution of 100 ng–0.01 ng of DNA. Each qPCR experiment consisted of at least 4 biological replicates with two technical replicates for each. Data were analysed according to the  $\Delta\Delta C_T$  method (Pfaffl, 2001). The expression level was normalized to two reference genes, VGSC (voltage-gated sodium channel, accession no. XM\_039435819.1) and Actin (accession no. EU179846.1). Data was visualized using GraphPad Prism v10 (GraphPad Software, USA).

### 2.5. Transgenic fly bioassays

Synthesised (Twist Bioscience) *CYP419A1* constructs were subcloned into the pUASTattB plasmid between EcoRI and XbaI sites. (GenBank: EF362409.1). Verified pUAST constructs were transformed by the fly facility at the University of Cambridge into the germline of a *D. melanogaster* strain, containing an attP docking site on chromosome 2 (attP40) and the phiC31 integrase gene under the control of the vasa regulatory region on the X chromosome (y w M (eGFP, vas-int, dmRFP) ZH-2A; P [CaryP]attP40) (Markstein et al., 2008), using the PhiC31 system. The resultant transgenic lines were balanced, and the integration of genes was confirmed by PCR and Sanger sequencing, as described previously (Manjon et al., 2018). Virgin females of the Act5C-GAL4 strain (y[1] w[\*]; P(Act5C-GAL4-w)E1/CyO) were crossed with UAS-*CYP419A1* males. Bioassays were used to test the susceptibility of the lines to insecticides using adult females. Five ethiprole concentrations (diluted in 50% acetone/water solution) were overlaid onto agar vials (1.5% agar, 1% sucrose, 4% acetic acid) and allowed to dry at room temperature overnight. Twenty adult female flies (2–7 days post-eclosion) were added to each vial with 5 vials per insecticide concentration. Mortality was assessed at 48h and 72h. Control mortality was assessed using agar vials overlaid with 50% acetone solution. LC<sub>50</sub> values, 95% fiducial limits and statistical analysis were calculated using the drc package (Ritz et al., 2015) in R Studio.

### 2.6. In silico data mining

*N. lugens* chromosome level genomic assemblies (GenBank: GCA\_014356525.1 and GCA\_015708395.1) available at the National Center for Biotechnology Information (NCBI) were interrogated for the presence of *CYP419A1* genomic locus using the inbuilt Geneious 10.2.3 (Biomatters, NZ) BLAST function using *CYP419A1* ORF as a query. Manual curation of intron-exon boundaries was also done using Geneious. For phylogenetic analysis, representative species of the major orders of insects (Subphylum: Hexapoda, Class: Insecta) were selected (Hemiptera, Hymenoptera, Lepidoptera, Coleoptera and Diptera). We also included representative species from 3 other Subphyla: Chelicerata (spiders, scorpions and mites); Myriapoda (millipedes and centipedes) and Crustacea (crustaceans). In total 42 species were included (Table S2). Mitochondrial clan P450 nucleotide sequences were retrieved from the NCBI databases with reference to P450 nomenclature used in Dermauw et al. (2020). To locate *CYP419A1*-related sequences the nucleotide sequence for *N. lugens* *CYP419A1* (KM217003) was used as a query in a BLASTn search initially gated by 'Insecta (taxid:50557)'

and then by 'Hemiptera (taxid:7524)'. To increase the number of BLAST hits the Transcriptome Shotgun Assembly (TSA) database was also interrogated for CYP419A1-related sequences. Where CYP419A1-related sequences were discovered, the TSA was interrogated to obtain other mitochondrial clan P450 sequences for the species. Incomplete sequences were not included. The remaining P450 nucleotide sequences were translated, and a multiple sequence alignment (MSA) was created using MUSCLE (Edgar, 2004) which was examined for the presence of the five conserved motifs associated with P450s. The P450s were named using the recognised P450 nomenclature (Nelson et al., 1993, 1996).

## 2.7. Phylogenetic analyses of mitochondrial clan P450s

The final set of mitochondrial P450 protein sequences was aligned with the outgroups *Pseudomonas putida* P450cam (UniProtKB/Swiss-Prot: P00183.2) and *Homo sapiens* CYP3A4 (UniProtKB/Swiss-Prot: P08684.4) in Geneious using MUSCLE (Edgar, 2004). MEGAX (Kumar et al., 2018) was used to determine the best-fit model of amino acid substitution, proportion of invariant sites and rate variation from the MSA, using a maximum likelihood fit of 56 different models. The substitution model with the lowest Bayesian Information Criteria score was selected for use in phylogeny estimation. The MSA was used to generate a phylogenetic tree using Bayesian inference (Huelsenbeck and Ronquist, 2001) (Substitution model: LG + G (Le and Gascuel, 2008); Chain length: 1,100,000; Subsampling frequency: 200; Burn-in length: 100,000; Heated chains: 4; Heated chain temperature: 0.2). The sequences from the CYP302, CYP419, CYP334 and CYP339 families were included with insect P450s known to lack the conserved cysteine residue in the heme-binding motif (the CTL-2 and CTL-6 groups (Dermauw et al., 2020)) in a second, more focused Bayesian inference (Huelsenbeck and Ronquist, 2001) phylogeny using PhyML (Guindon et al., 2010) (Substitution model: LG + G (Le and Gascuel, 2008); Chain length: 1,100,000; Subsampling frequency: 200; Burn-in length: 100,000; Heated chains: 4; Heated chain temperature: 0.2).

## 2.8. Modelling of CYP419 proteins to determine candidate amino acid residues involved in specificity and ligand transportation and binding

To identify specificity determining positions (SDPs) present in the CYP419 family of mitochondrial P450s, the SDPlight algorithm was used (Kalinina et al., 2004; Mazin et al., 2010). The CYP419 family was compared to all the other mitochondrial clan P450s used in the phylogeny to identify key amino acid residues that differed significantly between the two groups. Three-dimensional models of the two splice variants of *N. lugens* CYP419A1 were generated using AlphaFold2 (Mirdita et al., 2022; Jumper et al., 2021). The primary sequences were submitted to the ColabFold web interface (Mirdita et al., 2022) and the default options were chosen to run the software. Both available versions of ColabFold were used and, as such, the MSA step was performed with and without MMseqs2 (Mirdita et al., 2019). The stereochemical soundness and quality of the predicted models were assessed using the Structural Analysis and Verification Server (<https://saves.mbi.ucla.edu/>), and ERRAT scores (Colovos and Yeates, 1993), PROCHECK data (Laskowski et al., 1996) and Ramachandran plots were generated.

To predict the position of the heme molecule the AlphaFill database was searched to provide the closest available match to the models predicted in this study (Hekkelman et al., 2023). A *N. lugens* CYP419A1 sequence with an UniProt entry IDs already exists (Entry ID: A0A0K0LB73) and it was used to search the AlphaFill database (<http://alphafill.eu>) for an AlphaFold2 predicted model with associated ligands and co-factors. The models generated for this project were aligned with both AlphaFill models using Schrödinger Maestro Suite v13.3 (Schrödinger, USA), and alignment and RMSD scores were calculated (alignment scores CYP419A1 long splice variant and CYP419A1 short splice variant: 0.078 and 0.194 respectively). The models were refined

for further analysis by adding hydrogens, creating zero-order bonds to metals and disulphide bonds, and the heme iron (Fe) charge set to +3. The unusual heme-binding motif residues were examined for the presence of a hydrogen bond to the Fe<sup>3+</sup> in the heme molecule.

The prepared models were exported as 'holoenzymes' in a.pdb format and uploaded to Caver Web 1.1 for further analysis (Stourac et al., 2019). The volume (Å<sup>3</sup>), relevance score and druggability score of the catalytic pockets were estimated for each model before access tunnel detection was conducted. The structure of ethiprole was obtained from PubChem (compound CID: 99306667) and minimised in UCSF Chimera v 1.16 (Pettersen et al., 2004) (steepest descent steps: 1000; steepest descent step size: 0.02 Å; conjugate gradient steps: 100; conjugate descent step size: 0.02 Å). Subsequent transport analyses were conducted with ethiprole for all relevant access tunnels detected. Predicted tunnels were inspected for the inclusion of any residues highlighted using the SDPlight algorithm.

The holoenzymes were exported to UCSF Chimera v 1.16 and the secondary structure was examined with reference to the structures known to be implicated in binding and function in other P450s. In particular the F/G and B/C helix-rich regions and the I-helix were identified. The residues identified as making up the catalytic pockets by Caver Web 1.1 were also identified on the structures. Molecular docking was performed using AutoDock Vina 1.1.2 (Trott and Olson, 2010) to locate the potential binding position of ethiprole (minimised as before). For docking the grid size dimensions were fixed to 45 x 45 x 45 in the xyz axis and the grid was centred on the heme molecule. All other parameters were used as default set values. Docking poses were visualized in UCSF Chimera v 1.16.

## 3. Results

### 3.1. Alternatively spliced CYP419A1 is associated with ethiprole resistance in BPH

Analysis of RNAseq data generated in a previous study (Zimmer et al., 2018) identified the P450 gene *CYP419A1* as significantly over-expressed in ethiprole resistant strains of *N. lugens* in addition to the previously reported upregulation of *CYP6ER1* (Fig. 1). Specifically, *CYP419A1* was expressed at 6-fold higher levels in the ethiprole resistant NLF2 strain compared to the reference susceptible strain NLS. Furthermore, in a derivative of this strain that had been selected with ethiprole (NLF2eth) *CYP419A1* was expressed at 16-fold greater levels than observed in NLS, which translates to a 2.5-fold induction of expression upon further pesticide exposure. These results suggest that *CYP419A1* is associated with the resistant phenotype and is the second CYP gene after *CYP6ER1* to be implicated in resistance to ethiprole in BPH (Fig. 1).

### 3.2. CYP419A1 is a mitochondrial P450 with an unusual ORF

The coding sequence (CDS) of *CYP419A* in both resistant and susceptible strains was found to be contained on an unusually long transcript, with a theoretical ORF of 3810bp predicting a protein of 1269 AA (WT). It is not clear as to whether the sequence preceding P450 is just an extremely long 5'UTR or whether it is translated (Fig. 2A). However, the sequence is not disrupted by any stop codons and contains several methionine residues upstream of the predicted CYP region (Sup Fig. 1A). Moreover, the extremely long exon 1 was also found in other members of the Delphacidae family (Fig. 2B). Interrogation of the sequence upstream of the CYP region against sequence databases failed to return any hits for known functional domains and AlphaFold2 modelling did not show any structured conformation of the upstream region alone or when attached to the CYP (full-length 3810bp) ORF.

Interrogation of the publicly available genomic datasets (Ye et al., 2021) for *N. lugens* located the *CYP419A1* gene to the sub-telomeric region of Chromosome 11 (GenBank acc. no CM025315.1) and

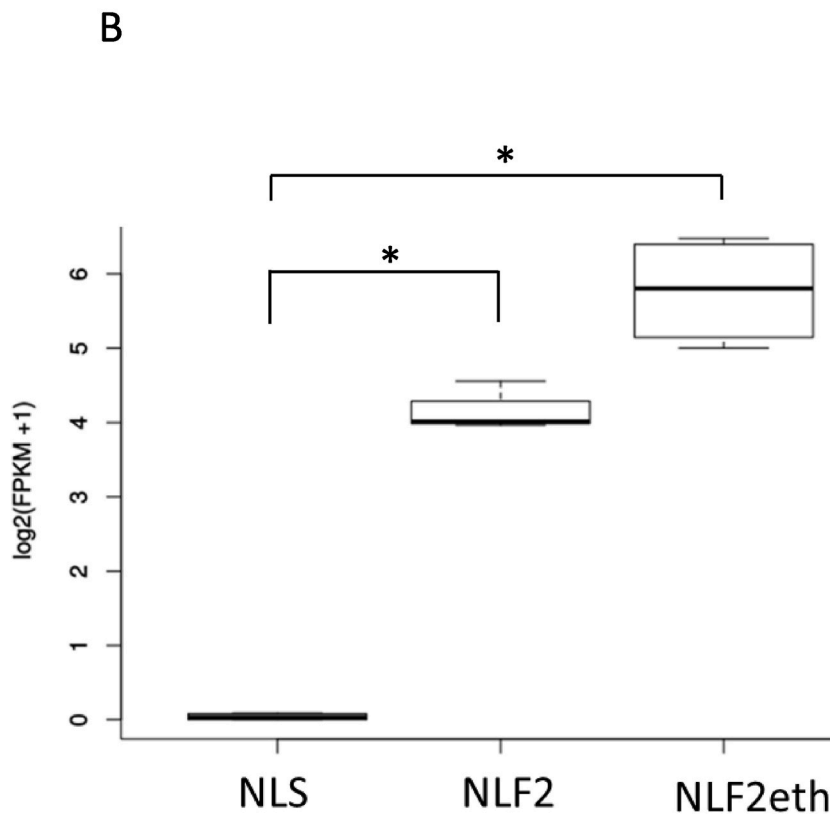
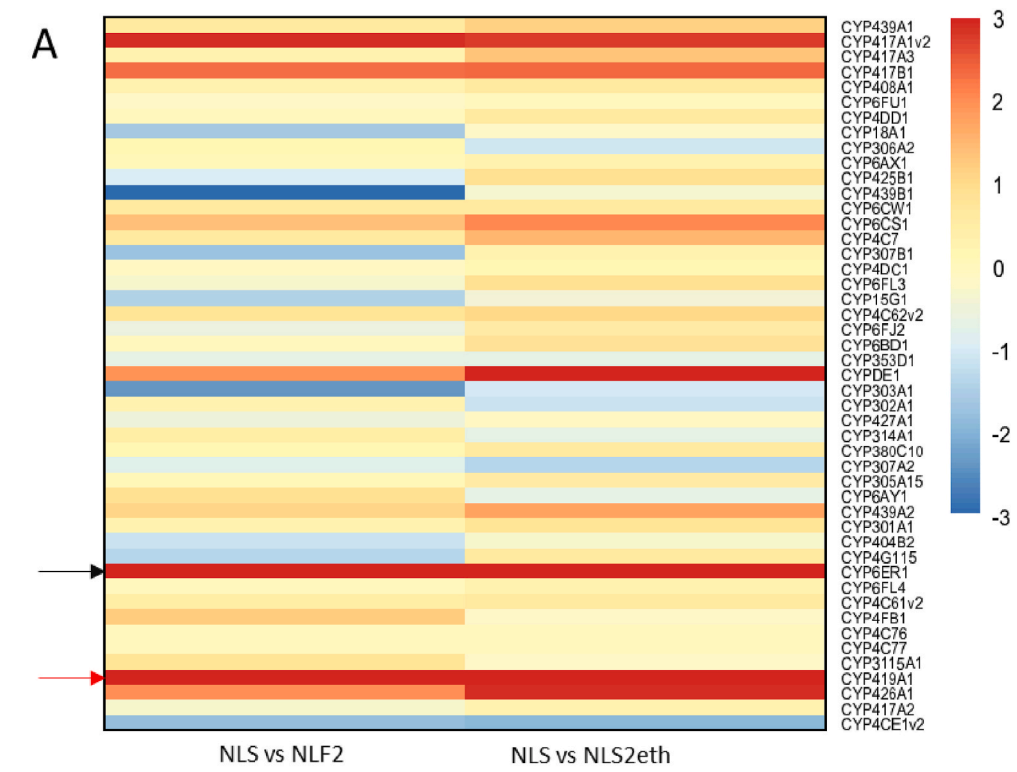


**Fig. 1.** Heat map of expression fold change (represented as LogFC) of the annotated CYP genes between the NLS and NLF2 and NLF2eth populations (Panel A) CYP6ER1 and CYP419A1 are indicated with black and red arrows. The mean FPKM value for CYP419A1 between NLS and NLF2 and NLF2eth, error bars represent standard error with the \* indicating p value of >0.05 (B). (For interpretation of the references to colour in this figure legend, the reader is referred to the Web version of this article.)

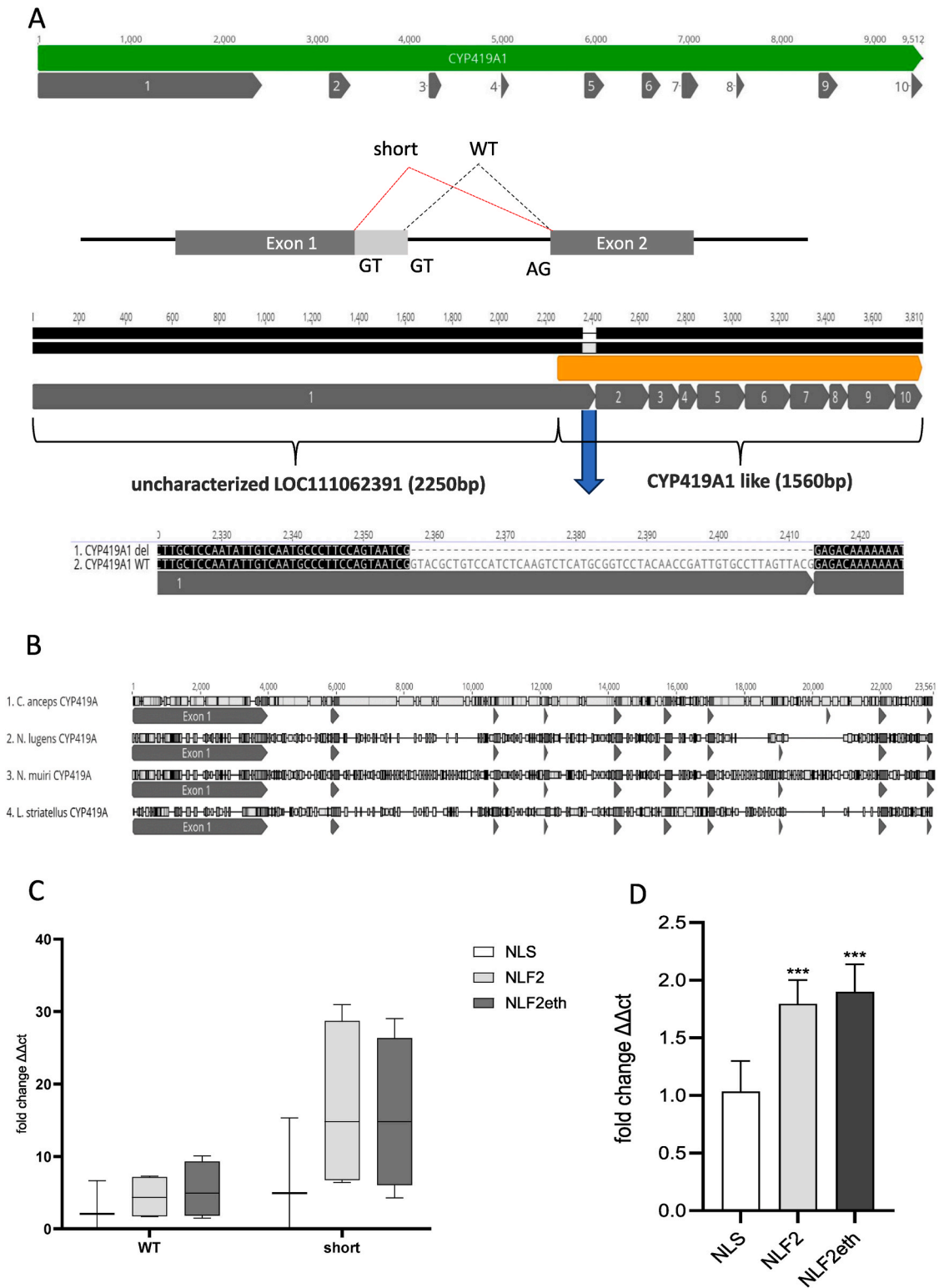


**Fig. 2.** Gene structure of CYP419A1 as assembled in CM027287.1 (chromosome 11) individual exons are shown as grey boxes followed by the assembled transcript with exon structure shown in grey. The predicted ORF of CYP419A1 is highlighted in orange. Mechanism of alternative splicing is proposed in the pane below, with both WT (black) and short splice versions (red) represented by dotted lines. The light grey box highlighted with a blue arrow indicates the region that is removed from CDS by alternative splicing in resistant populations. Close up sequence of this region indicates alternative splicing of the 3' end of exon 1 rather than a genomic deletion (A). Panel B shows multiple alignment of CYP419A1 with a complete gene locus from four representatives of Delphacidae. Extremely long exon 1 is found in all available species. Relative expression measured by qPCR of truncated and WT CYP419A1 in NLF2 and NLF2eth in comparison to NLS, error bars represent 95% confidence intervals, n = 4 (panel C). Gene copy number estimation measured by qPCR between NLS and NLF2 and NLF2eth error bars represent 95% confidence intervals, n = 8 (panel D). (For interpretation of the references to colour in this figure legend, the reader is referred to the Web version of this article.)

showed that it comprises 10 exons with an extremely long first exon. RT-PCR confirmed the large RNAseq assembled transcripts as genuine (sup Fig. 2B). Intriguingly, analysis of the *CYP419A1* transcripts in the ethiprole selected strain showed a ‘deletion’ of 57bp or 19AA from the 5’ end (N-term) portion of the P450 ORF/protein. This deletion was confirmed experimentally through RT-PCR done on both the NLF2 and NLF2 ethiprole selected strains. The ‘deletion’ identified in the NLF2 strain appears to be a result of alternative splicing of exon 1, with premature termination of exon 1 by a cryptic splice site (Fig. 2A). This was supported by analysis of DNA sequences which provided no evidence of the deletion at the DNA level. Investigation of the expression of the WT vs short transcripts using qPCR revealed that the shorter transcript is more highly expressed in the NLF2 and NLF2eth strains than the long transcript (Fig. 2C). Interestingly, the altered region of the transcript spans a portion of two regions: i) a hydrophobic rich and ii) putative mitochondrial targeting sequence, which are critical for successfully migrating the enzyme into the organelle (Ito et al., 1985) (Fig. 4A).

Copy number qPCR for the *CYP419A1* gene revealed there are 2 copies of the gene in the haploid genome of the NLF2 strain compared to a single copy in the susceptible control (Fig. 2D). Thus, the enhanced expression of this P450 gene in the resistant strain may be in part explained by copy number variation. This is further supported by published genomic data where two copies of *CYP419A1* can be found in at least one *N. lugens* strain (GenBank GCA\_014356525.1<sup>41</sup>), with both copies located on the same chromosome (11).

### 3.3. *CYP419A1* contributes to ethiprole resistance *in vivo*

To test whether *CYP419A1* contributes to ethiprole resistance *in vivo*, we generated a series of transgenic *D. melanogaster* lines carrying different versions of *CYP419A1*. Due to the extremely long predicted ORF, it is difficult to ascertain where the actual *CYP419A1* start codon is. The NCBI annotation of *CYP419A1* (Acc. no. AIW79966) is 658 AA long. However, the rationale for this annotation is unclear given the size of the transcript ORF. Therefore, we attempted to generate 4 lines: 2 with the full-length ORF (3810bp) with or without the deletion and two with only the P450 region as annotated by InterPro (1560bp). Only flies injected with a shortened version of *CYP419A1* ORF produced viable lines. Bioassays with both WT *CYP419A1* and the *CYP419A1del* showed modest, but significant, tolerance towards ethiprole but no significant resistance towards either fipronil or imidacloprid (Fig. 3, Table S3). Interestingly, the deletion does not appear to have any significant effect on enhancing ethiprole tolerance in *Drosophila*, suggesting it does affect the interaction of *CYP419A1* with ethiprole *in vivo*.

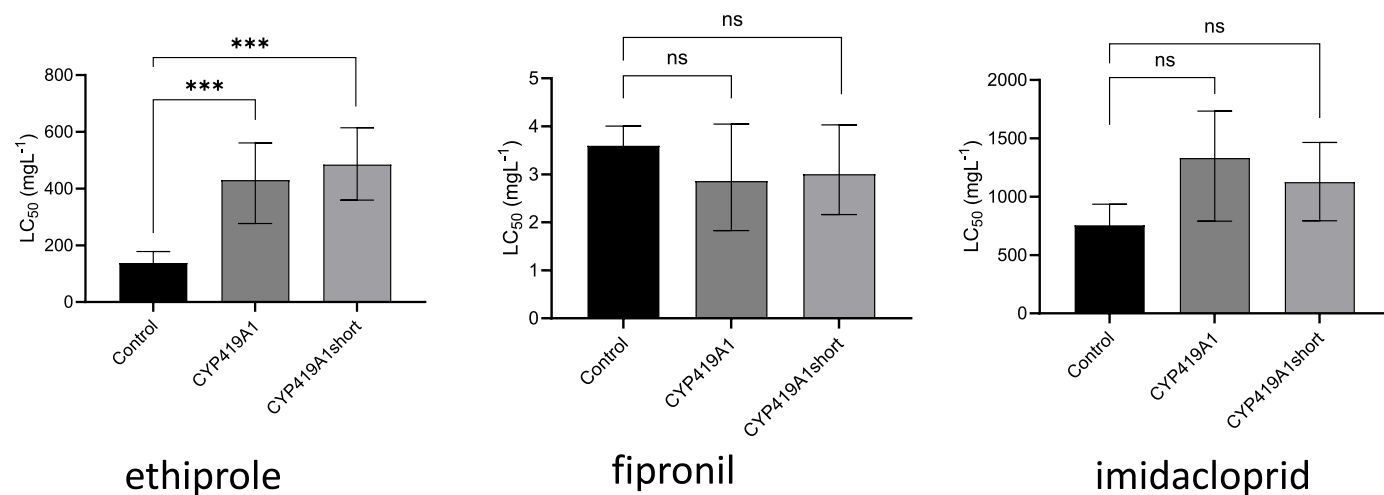


Fig. 3. Sensitivity of transgenic fly lines expressing either WT or deletion version of *CYP419A1* tested against 3 insecticides to which NLF2 exhibits enhanced tolerance: Ethiprole, Fipronil and Imidacloprid compared to empty vector control. Error bars represent 95% confidence intervals.

### 3.4. Modelling of *CYP419A1* variants shows unusual protein properties

AlphaFold2 modelling of WT *CYP419A1* and the *CYP419A1del* mutant showed conformational changes at the site of the deletion as well as in two outlying regions (Fig. 4B and C). Both models provided good ERRAT scores and Ramachandran plots (Fig. S3). Active site and docking analysis with ethiprole for predicted structures using CAVER (Table S4) showed that both splice versions have predominantly high (positive)  $E_{max}$  and  $E_a$  values ( $>20$  kcal/mol), which indicates a high energy barrier to movement through the access tunnels from the surface. Conversely, tunnel entrances in both versions have low (negative) surface binding values -  $E_{surface}$  (-6.8 WT and -4.6 DELKcal/mol). This suggests that ethiprole may bind at the surface but not move through the enzyme to the active site. The major difference between the two splice variants is that the long version has a high energy barrier to ethiprole binding at the active site (positive  $E_{bound}$   $>10$  kcal/mol). Whereas the short version has predominantly negative  $E_{bound}$  values which indicate that if ethiprole could move through the access tunnels it would be bound and potentially metabolised (Table S4). However, it is important to acknowledge that binding the substrate, CPR (or another co-factor) might create conformational change, thereby ‘opening’ some of the tunnels to facilitate movement.

In the canonical heme-binding motif of a P450, a highly conserved cysteine (CYS) provides the thiolate ligand to the heme molecule. In the *CYP419* family, however, there is a substitution of phenylalanine (PHE) for the CYS at position 466 (WT) (Fig. 6). The AlphaFold2 modelling indicates the formation of a hydrogen bond between the iron atom of the heme and the aromatic ring in the side chain of PHE466.

### 3.5. Phylogenetic analyses of *CYP419A1* shows family specificity to the infra-order Fulgoromorpha (planthoppers)

In all we retrieved 272 mitochondrial P450 sequences from 42 species (Table S2). The resulting phylogeny performed using Bayesian inference (Fig. 5A) revealed ten distinct gene lineages: CYP3118, CYP12/333/428, CYP301/49, CYP315, CYP314, CYP335/353/363, CYP44/404, CYP302, CYP362/3674 and CYP334/339/419. The majority of the nodes in the phylogeny had strong Bayesian posterior probability support ( $>80\%$ ). Although the support values dropped for some of the deeper nodes, where more uncertainty is expected, none were lower than 51%.

The CYP302, CYP314 and CYP315 gene families appear to be present in all the Subphyla of arthropods included in the phylogeny. Whereas, other lineages are insect-specific, for example, the CYP301 and CYP49

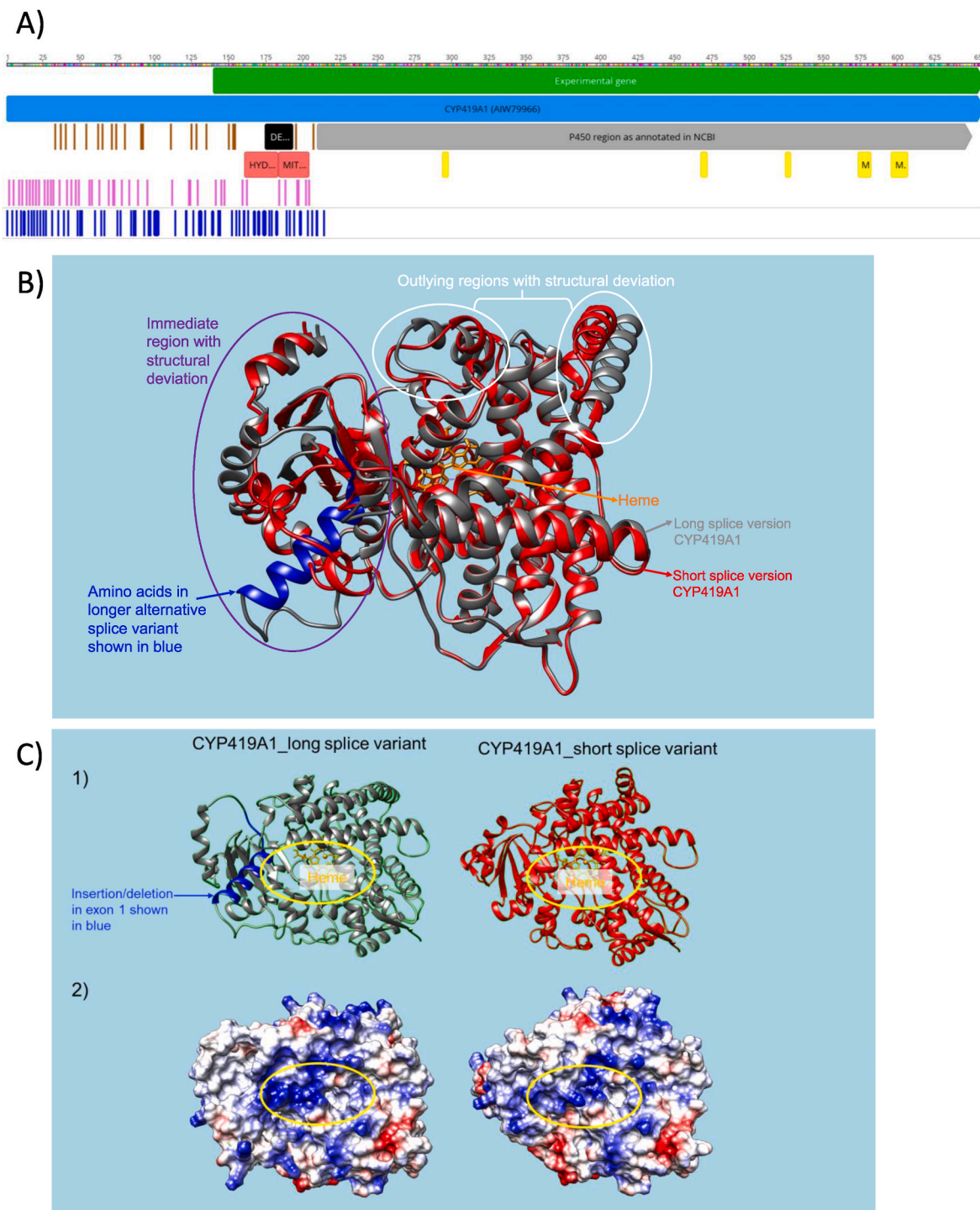


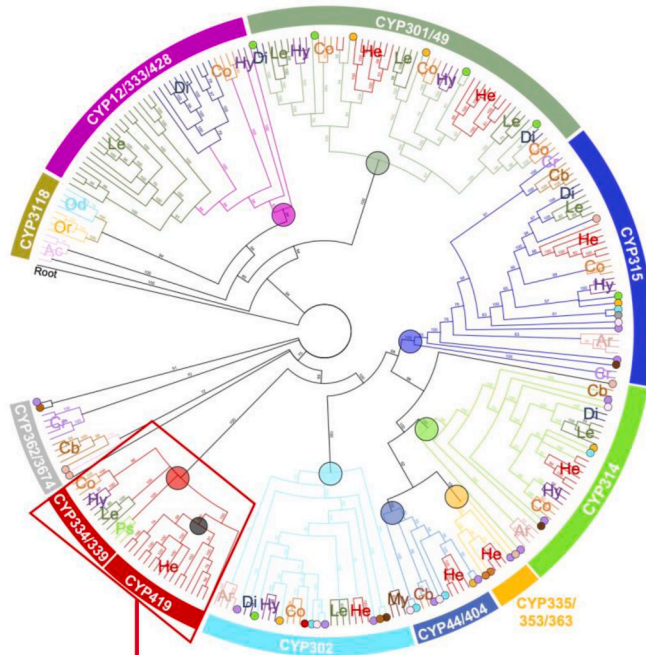
**Fig. 4.** Graphical representation of CYP419A1 protein sequence as it is annotated in NCBI (acc. No. AIW79966 in light blue). The grey bar represents the cytochrome P450 domain as recognised by NCBI feature search with substrate recognition sites in yellow. The green bar represents the experimental P450 sequence used in this study. Individual lines correspond to (blue) hydrophobic, positively charged (pink) and negatively charged (brown) amino acids. The proposed hydrophobic rich and mitochondrial signal regions are marked in red, while the region removed by alternative splicing is marked in black (A). Image generated using Schrodinger's Maestro, overlaying and highlighting divergent protein regions between two variants (B). Panel C shows: (top 1) Secondary structure of CYP419A1 splice variants (long and short). Heme molecule is shown in orange and the insertion/deletion observed in exon 1 is coloured in blue. 2): Protein surface overlaid with electrostatic potential. Putative position of access tunnels entrance in (A) and (B) marked with yellow ellipse. Figure created using UCSF Chimera version 1.16. (For interpretation of the references to colour in this figure legend, the reader is referred to the Web version of this article.)

gene families, which share a recent common ancestor. There is evidence for a duplication event within the CYP314 family, giving rise to the CYP335/353/363 and CYP44/404 lineages in certain groups of arthropods, including Collembola, Hexanauplia, Branchiopoda, Malacostraca and Arachnida, as well as several orders of insects (Archaeognatha,

Odonata, Orthoptera, Hemiptera and Coleoptera).

The CYP419 family only appears to be present in the superfamily Fulgoromorpha (planthoppers) and is not present in the other Hemipteran species. A focused phylogenetic analysis of two groups of unusual CYS-less P450s and those gene families that share a common ancestor

A



Nodes:

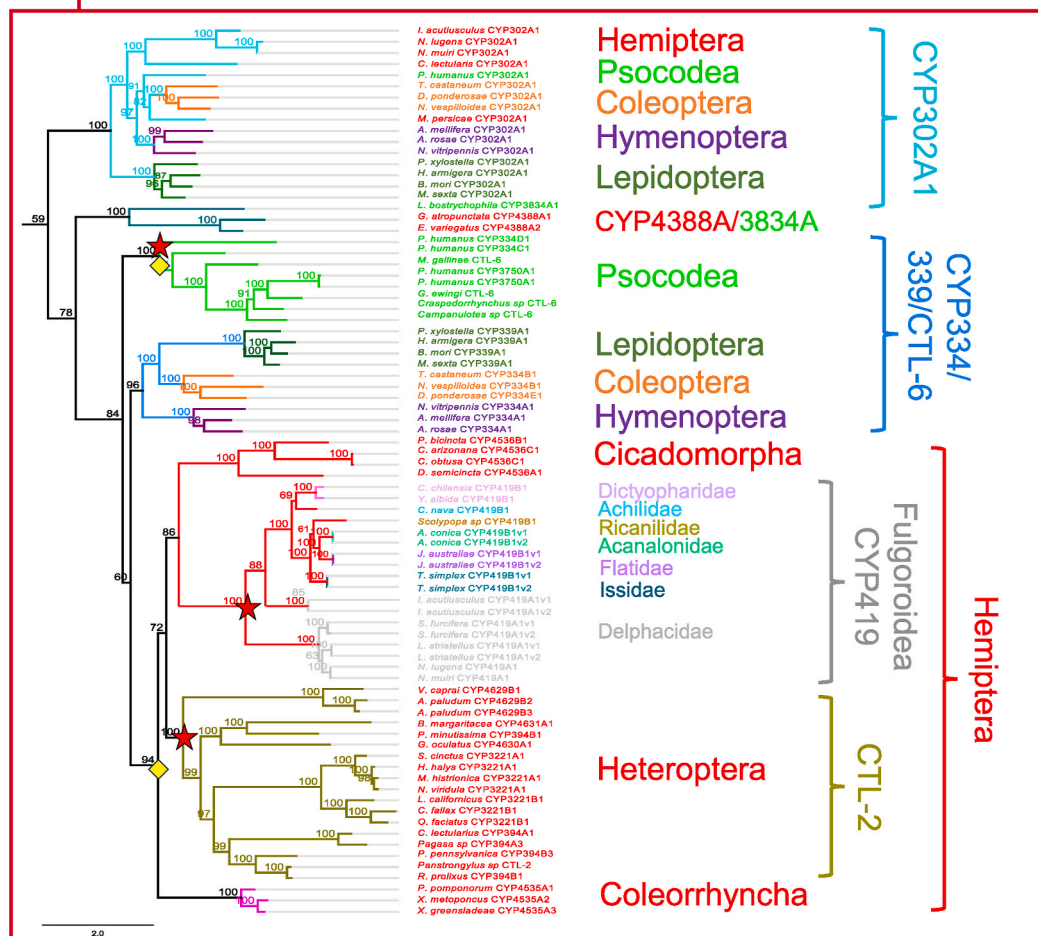
- CYP12/333/428
- CYP301A/301B/49
- CYP315
- CYP314
- CYP335/353/363
- CYP44/404
- CYP302
- CYP334/339/419
- Fulgoroidea - planthoppers

Taxonomic group:

- Cr Crustacea
- My Myriapoda
- Cb Collembola
- Ar Arachnida
- Od Odonata
- Or Orthoptera
- Ac Archaeognatha
- Ps Psocoda
- Zy Zygentoma
- He Hemiptera
- Hy Hymenoptera
- Co Coleoptera
- Le Lepidoptera
- Di Diptera

Arthropods  
Insects

B



(caption on next page)



**Fig. 5.** Phylogenetic analysis of the evolutionary origin of the CYP419 family of P450s in arthropods. (A) Phylogeny of the mitochondrial clan of P450s from 42 species of arthropod showing the major gene families. (B) Phylogenetic relationship of the CYP419 family to other non-canonical insect mitochondrial clan P450s and the CYP334/339 family. P450s were aligned with the outgroup *P. putida* P450cam (UniProtKB/Swiss-Prot: P00183.2) and *H. sapiens* CYP3A4 (UniProtKB/Swiss-Prot: P08684.4) in Geneious 10.2.3 (Biomatters) using MUSCLE (Edgar, 2004). Amino acid substitution was modelled using the LG matrix (Le and Gascuel, 2008). Phylogeny estimated with Bayesian inference (chain length, 1,100,000; subsampling frequency, 200; burn-in length, 100,000; heated chains, 4; heated chain temperature, 0.2). Posterior probability (%) shown on nodes. (A): Abbreviated names of taxonomic groups: Cr, Crustacea; My, Myriapoda; Cb, Collembola; Ar, Arachnida; Od, Odonata; Or, Orthoptera; Ac, Archaeognatha; Ps, Psocodea; Zy, Zygentoma; He, Hemiptera; Hy, Hymenoptera; Co, Coleoptera; Le, Lepidoptera; Di, Diptera. (B) Species included: Hymenoptera: *Apis mellifera*, *Athalia rosae*, *Nasonia vitripennis*, Coleoptera: *Dendroctonus ponderosa*, *Nicrophorus vespilloides*, *Tribolium castaneum*, Lepidoptera: *Bombyx mori*, *Helicoverpa armigera*, *Manduca sexta*, *Plutella xylostella*, Hemiptera: *Acanalonia conica*, *Aquarius paludum*, *Buenoa margaritacea*, *Catantopius nava*, *Chauliops fallax*, *Chondrodire chilensis*, *Cimex lectularius*, *Clastoptera arizonana*, *Clastoptera obtusa*, *Diceroprocta semicincta*, *Euscelidius variegatus*, *Gelastocoris oculatus*, *Graphocephala atropunctata*, *Halyomorpha halys*, *Idiosystatus acutiusculus*, *Jamella australiae*, *Laodelphax striatellus*, *Largus californicus*, *Murgantia histrionica*, *Myzus persicae*, *Nezara viridula*, *Nilaparvata lugens*, *Nilaparvata mui*, *Oncopeltus fasciatus*, *Pagasa* sp., *Panstrongylus* sp., *Peloidium pomponorum*, *Phymata pennsylvanica*, *Plea minutissima*, *Prosapia bicinta*, *Rhodnius prolixus*, *Scolypopa* sp., *Sehirus cinctus*, *Sogatella furcifera*, *Thionia simplex*, *Velia caprai*, *Xenophyes metoponcus*, *Xenophysella greensladeae*, *Yucanda albida*, Psocodea: *Campanulotes* sp., *Craspedorrhynchus* sp., *Geomydoecus ewingi*, *Menopon gallinae*, *Pediculus humanum*. Red star indicates ancestral node of CYS-less heme-binding motif, yellow diamond indicates ancestral node of loss of WxxxR motif. (For interpretation of the references to colour in this figure legend, the reader is referred to the Web version of this article.)

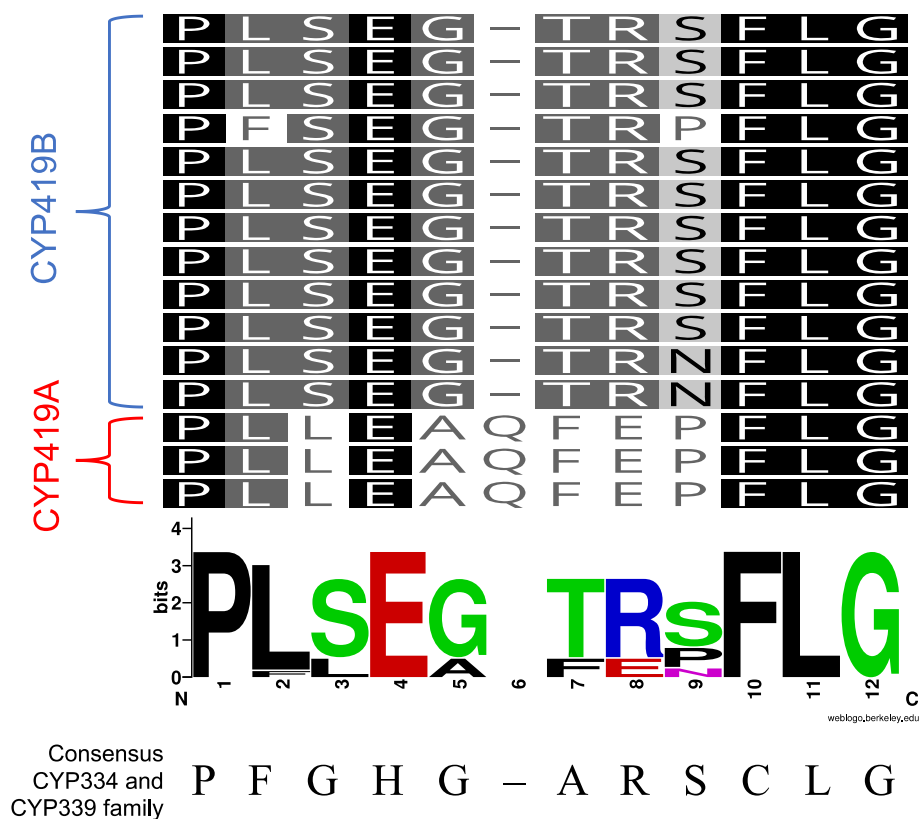


**Fig. 6.** Binding motif of the CYP419 family lacking the conserved CYS. Multiple sequence alignment of the heme-binding motif of the CYP419A and CYP419B subfamilies, with the consensus sequence produced by Weblogo (Crooks et al., 2004) shown below. The consensus sequence for CYP334 and CYP339 families of P450s is shown in plain type below.

with the Fulgoromorpha-specific CYP419s was performed to elucidate the evolutionary relationship within the clade. The resulting phylogeny has good posterior probability support with most nodes >80% (Fig. 5B). The CYP419 family is found in seven families of planthoppers and is composed of two subfamilies, CYP419A and CYP419B. The closest hemipteran sequences in the phylogenetic analyses are the CYP4536 family, which is found in the Cicadomorpha (cicadas, leafhoppers and spittle bugs), which share a common ancestor with the Fulgoromorpha. The type 2 CYS-less (CTL-2) sequences, present in certain Heteroptera species, form a sister group to the CYP419 and CYP4536 sequences. Together these sequences form a clade of hemipteran P450s with non-typical heme-binding motifs. The CTL-2 and CYP419 families both lacking the conserved cystine and the CYP4536 having a cystine offset by two amino acids, resulting in a non-typical cystine loop. However, the CYP4535A family, present in the Coleorrhyncha (a suborder that

diverged after the Heteroptera), has a canonical heme-binding motif and forms a sister group to these non-typical P450s, which implies that the CYS-less heme-binding motifs found in the CTL-2 sequences arose independently from those present in the CYP419 family. Whereas the loss of the canonical WxxxR motif appears to have arisen before the divergence of the CTL-2, CYP419, CYP4536 and CYP4535 sequences.

The CYP334 and CYP339 gene families share a common ancestor with the CYP419, CTL-2, CYP4535 and CYP4536 P450s. In the Lepidoptera, Coleoptera and Hymenoptera these P450s have canonical conserved motifs. Whereas CYP334D1, present in the Psocodea species, *Pediculus humanus* (body louse), has a non-typical heme-binding motif and clades with another group of CYS-less P450s, the CTL-6s. The evolution of this non-canonical heme-binding motif again appears to have arisen independently of the CTL-2 and CYP419s. CYP334 and CYP339 are insect-specific, although they are not ubiquitous across all insect

orders. Both families appear to be absent in Diptera, Archaeognatha, Zygentoma, Odonata, Orthoptera and many hemipteran species (particularly the Sternorrhyncha). It appears likely therefore that the common ancestor of the CYP419, CYP334 and CYP339 gene families arose after the Neoptera diverged from the other insect taxa.

Brief interrogation of the NCBI assembled transcriptomes database (TSA) for the Fulgoroidea showed that outside of Delphacidae, other members of the subfamily show evidence of CYP419 like protein although overall homology is low with the top scoring hits of 47.39% from *Cyrpoptus belfragei* (family Fulgoridae). The transcripts for these proteins also appear quite large (*C. belfragei* 2581bp) with the longest predicted ORF of 2097bp. All identified CYP419 P450s have an unusual heme-binding motif. This ancestral gene subsequently evolved into the distinct gene families we see today but has since been lost in the Diptera and some species of Hemiptera.

#### 4. Discussion

Our data identified a P450 of the mitochondrial clan that is over-expressed in ethiprole resistant strains of *N. lugens* and has the capacity to confer resistance to this compound *in vivo*. This P450 has several unusual features including altered splicing associated with resistance, a non-canonical heme-binding motif and an extreme 5' end extension of the open reading frame. We discuss these topics below.

The identification of the role of CYP419A1 in ethiprole resistance in our study represents the second P450 after CYP6ER1 to be implicated in resistance to this compound in *N. lugens*. Flies expressing CYP419A1 had a resistance ratio (RR) of 3.5 (del) and 3.1 (WT) in comparison to empty vector control when exposed to ethiprole. In comparison flies expressing CYP6ER1vA in a previous study (Duarte et al., 2022) have a RR of 7.71 while the K176T variant of ER1vA had a resistance ratio of 15.4. Given that the NLF2 strain already overexpresses certain allelic variants of CYP6ER1 (Zimmer et al., 2018; Duarte et al., 2022) at a much higher level; this comparatively modest (around 6-fold) overexpression is likely to be an accessory mechanism further augmenting the resistant phenotype. However, in future it would be interesting to confirm the relative contribution of CYP419A1 and CYP6ER1 to the resistant phenotypes observed in *N. lugens* and understand if they act additively or synergistically. The expression of CYP419A1 is further enhanced by continuous exposure to ethiprole. The ectopic overexpression of two CYP419A1 transcript variants in transgenic fruit flies results in their enhanced tolerance to ethiprole revealing their direct contribution to resistant phenotype *in vivo*. In combination, these findings provide an example of how strong insecticide selection can lead to the co-overexpression of more than one P450 in resistant insects as has been described previously in mosquitoes and houseflies (Li et al., 2023; Yang et al., 2021).

Although P450s are one of the key enzymes involved in insecticide detoxification leading to phenotypic resistance, direct involvement of genes from the mitochondrial clan has not been historically observed often. In *Drosophila* spp. the mitochondrial P450 CYP12A4 and its chimeric variants CYP12A4/5 are associated with lufenuron resistance (Bogwitz et al., 2005; Good et al., 2014). However, ubiquitous overexpression of CYP12A4 results in embryonic lethality suggesting it may have some function during embryogenesis (Bogwitz et al., 2005). In insecticide-resistant *Musca domestica*, CYP12A1 was found to be constitutively overexpressed (approx. 5-fold), with heterologously expressed enzyme showing some activity against tested insecticides (Guzov et al., 1998). Recently more examples of direct or potential involvement of mitochondrial CYP genes in insecticide detoxification have been emerging in the literature. In the small brown planthopper, *Laodelphax striatellus* overexpressed CYP353D1v2 was shown to metabolise imidacloprid *in vitro*, with a microsomal CPR as a redox partner, suggesting the potential for it to be bimodal (Elzaki et al., 2017; Xu et al., 2020). Interestingly, CYP419A1 from the same species was also implicated in triflumezopyrim susceptibility through RNAi mediated knockdown, the authors however do not report on the unusual features

of CYP419A1 despite attempting molecular docking (Wang et al., 2023). CYP339A1 from *Spodoptera litura* expressed in transgenic flies has also been associated with indoxacarb resistance (Li et al., 2024). In the common pest of mulberry *Glyphodes pyloalis* RNAi knockdown of CYP333A36 increased susceptibility of the insect to tolfenpyrad (Pan et al., 2023). A recent study of the mitochondrial and CYP2 clans in *Helicoverpa armigera* demonstrated that members of the mitochondrial clan, CYP339A1 and CYP305B1, can hydrolyse the pyrethroid esfenvalerate while CYP333B3 can epoxidize aldrin (Shi et al., 2022). Although the study clearly showed that insect mitochondrial P450s can interact with insecticides, it did not establish a direct association to field evolved resistance to aldrin or pyrethroids in *H. armigera*. In the Asian honey bee, *Apis cerana* expression of CYP315A1 and CYP301A1 is induced by compounds belonging to the neonicotinoid, pyrethroid and organophosphate classes of insecticides (Zhang et al., 2019) and, in the case of CYP301A1, RNAi mediated knockdown results in increased mortality upon exposure to insecticides (Zhang et al., 2019).

Many P450s classified as mitochondrial clan members are identified as such through phylogeny, rather than direct evidence of expression in mitochondria (Dermauw et al., 2020). Only a few CYP genes that clade with the mitochondrial clan have been experimentally shown to utilise Adx-AdR redox partners rather than CPR, and these exemplars are only from a limited number of species (Guzov et al., 1998; Shi et al., 2022). There is growing evidence that some microsomal P450 proteins show bimodal targeting to both endoplasmic reticulum and mitochondria (Sangar et al., 2010). The NLF2 strain expresses a splice variant of CYP419A1, which is likely to be missing a key portion of the putative mitochondrial signal peptide thus trapping the expressed protein outside of the mitochondria. Since the 3D models do not show any clear N-terminal anchor domain, we speculate that in the resistant *N. lugens* this protein remains in the cytosol. Given that both variants of the CYP419A1 exhibit similar level of protection against ethiprole in transgenic *D. melanogaster*, and the molecular docking studies do not support good transport to the active site of the enzymes, it is possible that CYP419A1 acts by insecticide sequestration rather than direct metabolism. Overexpression of sequestering carboxylesterase proteins is one of the key mechanisms of organophosphate resistance in *Myzus persicae* (Devonshire and Moores, 1982), although the level of overexpression in that case is an order of magnitudes higher (Field et al., 1996) than those reported here.

An atypical feature of the coding sequence of CYP419A in both the resistant and susceptible strains of *N. lugens* analysed in this study is that it is contained on an unusually long transcript, due to a long ORF that precedes the region encoding known P450 domains. Transcriptomic analysis confirmed that the entire region is transcribed, however, it is unclear if or how much of the upstream region is translated. Indeed, this region contains multiple methionine residues that might serve as start codons to initiate translation. Our interrogation of this region against sequence databases failed to return any hits for known functional domains and AlphaFold2 modelling did not show any structured conformation. However, interrogation of the genomes of other hopper species identified a similar region upstream of orthologs of CYP419A suggesting it predates divergence of these hopper species and may have been retained due to functional constraint. Our attempts to functionally investigate proteins with this domain in *D. melanogaster* proved unfruitful as we failed to generate viable transformants from flies injected with the full-length transcript. Thus, further work is warranted to investigate this ORF in more detail either using *in vitro* approaches and/or via genetic modification of *N. lugens* using CRISPR-Cas genome editing (Zhang et al., 2023).

We also demonstrate that CYP419A1 is duplicated in ethiprole resistant strains of *N. lugens*. This may in part explain the overexpression of this P450 gene in resistant strains as a result of its effect on gene dosage. This finding has parallels with research on CYP6ER1 which was also found to be duplicated in resistant strains (Zimmer et al., 2018). In the same study, divergence in the expression of CYP6ER1 copies was

identified in resistant strains with the copy carrying mutations that are key to insecticide detoxification overexpressed (Zimmer et al., 2018). In our study we observed similar asymmetry in the expression of *CYP419A1* copies, with the altered splice form lacking the mitochondrial signal peptide expressed at higher levels than the wildtype copy. Identification of the mutation(s) leading to this divergence in expression, and its functional significance, requires further work. However, as noted above the altered and wild-type isoforms confer the same levels of ethiprole resistance when ectopically expressed in *D. melanogaster*. Thus, selection for overexpression of the altered splice form of *CYP419A1* may be linked to its effect on cellular localisation.

The structure of *CYP419A1* is unusual as it lacks the highly conserved cysteine residue that is often seen as one of the signatures of the P450 superfamily and is responsible for proximal co-ordination of the heme iron. This interaction is critical to the spectral shift to 450 nm upon exposure to carbon monoxide in the active form of the enzyme which gives the basis for its name (Munro et al., 2018). Replacement of the conserved cysteine has been shown to result in alterations to the biochemical properties of P450 2B4, with a shift in Soret maxima and almost complete loss of monooxygenase activity (Vatsis et al., 2002). *CYP419* sequences also lack the conserved WxxxR motif found in the C-helix in canonical P450s. The highly conserved arginine (R) in this motif is thought to stabilise the propionate of the heme (Feyereisen, 2012). Although our modelling data suggests that in *CYP419A1* PHE466 is interacting with the heme iron in place of a cysteine residue, we cannot fully discount the possibility that these proteins are unable to successfully bind heme.

Since the endogenous function of *CYP419A1* in *N. lugens* is unknown and the entire gene subfamily appears to well conserved and specific to planthoppers, we speculate that this gene has evolved in response to some ecologically specific challenge faced by this group of insects.

Whilst the lack of a conserved cysteine that provides the thiolate bond to the heme is unusual, it has evolved independently on at least six occasions in arthropods (Dermauw et al., 2020). Indeed, the mitochondrial CTL-2 and CTL-6 sequences (included in our phylogeny) have no recognisable heme-binding motif (Dermauw et al., 2020). Several different residues have been shown to replace the canonical cysteine, such as serine, tyrosine, histidine and aspartic acid (Dermauw et al., 2020), but this is the first instance where phenylalanine is implicated in the stabilization of the heme molecule in a P450. The functions of the CYS-less P450s identified are unknown, but mutated P450s, with either histidine or serine in place of cysteine, have carbene- and nitrene-transfer activity (McIntosh et al., 2015). It seems likely therefore, that new P450-activities and chemistries may be uncovered as the biochemical profiles of these unusual enzymes are studied. Further biochemical work is also required to determine the spectral shift that has occurred in the Soret peak due to the C-HEME-F substitution. It has been established that CYS-less mutants produce altered Soret peaks, for example the *CYP119* mutant C317H bound with CO has a peak of 422 nm (McIntosh et al., 2015).

In summary, our work in combination with previous studies (Zimmer et al., 2018; Duarte et al., 2022) reveal how insecticide resistance can be mediated by quantitative and qualitative changes in multiple P450s involving a diverse array of mutations. Our data also provide new insight into the under investigated P450s of the insect mitochondrial clan and their role in xenobiotic detoxification.

#### CRedit authorship contribution statement

**B. Zeng:** Validation, Investigation, Formal analysis, Data curation. **A.J. Hayward:** Writing – review & editing, Visualization, Software, Methodology, Investigation, Formal analysis, Data curation. **A. Pym:** Visualization, Software, Data curation. **A. Duarte:** Methodology, Formal analysis, Data curation. **W.T. Garrood:** Writing – review & editing, Software, Data curation. **S-F Wu:** Writing – review & editing, Supervision. **C-F Gao:** Writing – review & editing, Supervision. **C. Zimmer:**

Writing – review & editing, Investigation, Data curation. **M. Mallott:** Supervision, Methodology, Investigation. **T.G.E. Davies:** Writing – review & editing, Resources, Funding acquisition. **R. Nauen:** Writing – review & editing, Supervision, Resources. **C. Bass:** Writing – review & editing, Resources, Project administration, Funding acquisition. **B.J. Troczka:** Writing – review & editing, Writing – original draft, Data curation.

#### Acknowledgements

For the purpose open access, the author has applied a ‘Creative Commons Attribution (CC BY) license to any Author Accepted Manuscript version arising from this submission. Rothamsted Research receives strategic funding from the Biotechnology and Biological Sciences Research Council of the United Kingdom (BBSRC). We acknowledge support from the Growing Health Institute Strategic Programme [BB/X010953/1; BBS/E/RH/230003A]. Troczka B. was funded by BBSRC Discovery Fellowship grant no. BB/X010058/1. We also want to thank Professor Rene Feyereisen for advice, ideas and support in drafting the final version of the manuscript.

#### Appendix A. Supplementary data

Supplementary data to this article can be found online at <https://doi.org/10.1016/j.ibmb.2025.104260>.

#### Data availability

Data will be made available on request.

#### References

- Bogwitz, M.R., et al., 2005. *Cyp12a4* confers lufenuron resistance in a natural population of *Drosophila melanogaster*. *Proc Natl Acad Sci U S A* 102, 12807–12812. <https://doi.org/10.1073/pnas.0503709102>.
- Caboni, P., Sammelson, R.E., Casida, J.E., 2003. Phenylpyrazole insecticide photochemistry, metabolism, and GABAergic action: ethiprole compared with fipronil. *J. Agric. Food Chem.* 51, 7055–7061. <https://doi.org/10.1021/jf030439l>.
- Cole, L.M., Nicholson, R.A., Casida, J.E., 1993. Action of phenylpyrazole insecticides at the GABA-gated chloride channel. *Pestic. Biochem. Physiol.* 46, 47–54. <https://doi.org/10.1006/pest.1993.1035>.
- Colovos, C., Yeates, T.O., 1993. Verification of protein structures: patterns of nonbonded atomic interactions. *Protein Sci.* 2, 1511–1519. <https://doi.org/10.1002/pro.5560020916>.
- Crooks, G.E., Hon, G., Chandonia, J.M., Brenner, S.E., 2004. WebLogo: a sequence logo generator. *Genome Res.* 14, 1188–1190. <https://doi.org/10.1101/gr.849004>.
- Dermauw, W., Van Leeuwen, T., Feyereisen, R., 2020. Diversity and evolution of the P450 family in arthropods. *Insect Biochem. Mol. Biol.* 127, 103490. <https://doi.org/10.1016/j.ibmb.2020.103490>.
- Devonshire, A.L., Moores, G.D., 1982. A carboxylesterase with broad substrate specificity causes organophosphorus, carbamate and pyrethroid resistance in peach-potato aphids (*Myzus persicae*). *Pestic. Biochem. Physiol.* 18, 235–246. [https://doi.org/10.1016/0048-3575\(82\)90110-9](https://doi.org/10.1016/0048-3575(82)90110-9).
- Duarte, A., et al., 2022. P450 gene duplication and divergence led to the evolution of dual novel functions and insecticide cross-resistance in the brown planthopper *Nilaparvata lugens*. *PLoS Genet.* 18, e1010279. <https://doi.org/10.1371/journal.pgen.1010279>.
- Edgar, R.C., 2004. MUSCLE: multiple sequence alignment with high accuracy and high throughput. *Nucleic Acids Res.* 32, 1792–1797. <https://doi.org/10.1093/nar/gkh340>.
- Elzaki, M.E.A., et al., 2017. Imidacloprid is degraded by *CYP353D1v2*, a cytochrome P450 overexpressed in a resistant strain of *Laodelphax striatellus*. *Pest Manag. Sci.* 73, 1358–1363. <https://doi.org/10.1002/ps.4570>.
- Field, L.M., Devonshire, A.L., Tyler-Smith, C., 1996. Analysis of amplicons containing the esterase genes responsible for insecticide resistance in the peach-potato aphid *Myzus persicae* (Sulzer). *Biochem. J.* 313 (Pt 2), 543–547. <https://doi.org/10.1042/bj3130543>.
- Garrood, W.T., et al., 2016. Field-evolved resistance to imidacloprid and ethiprole in populations of brown planthopper *Nilaparvata lugens* collected from across South and East Asia. *Pest Manag. Sci.* 72, 140–149. <https://doi.org/10.1002/ps.3980>.
- Garrood, W.T., et al., 2017. Influence of the RDL A301S mutation in the brown planthopper *Nilaparvata lugens* on the activity of phenylpyrazole insecticides. *Pestic. Biochem. Physiol.* 142, 1–8. <https://doi.org/10.1016/j.pestbp.2017.01.007>.
- Good, R.T., et al., 2014. The molecular evolution of cytochrome P450 genes within and between *Drosophila* species. *Genome Biol Evol* 6, 1118–1134. <https://doi.org/10.1093/gbe/evu083>.

- Guindon, S., et al., 2010. New algorithms and methods to estimate maximum-likelihood phylogenies: assessing the performance of PhyML 3.0. *Syst. Biol.* 59, 307–321. <https://doi.org/10.1093/sysbio/syq010>.
- Guzov, V.M., Unnithan, G.C., Chernogolov, A.A., Feyereisen, R., 1998. CYP12A1, a mitochondrial cytochrome P450 from the house fly. *Arch. Biochem. Biophys.* 359, 231–240. <https://doi.org/10.1006/abbi.1998.0901>.
- Hamada, A., Stam, L., Nakao, T., Kawashima, M., Banba, S., 2020. Differential metabolism of neonicotinoids by brown planthopper, *Nilaparvata lugens*, CYP6ER1 variants. *Pestic. Biochem. Physiol.* 165, 104538. <https://doi.org/10.1016/j.pestbp.2020.02.004>.
- Health, E.P.o.P., et al., 2023. Pest categorisation of *Nilaparvata lugens*. *EFSA J.* 21, e07999. <https://doi.org/10.2903/j.efsa.2023.7999>.
- Hekkelman, M.L., de Vries, I., Joosten, R.P., Perrakis, A., 2023. AlphaFold: enriching AlphaFold models with ligands and cofactors. *Nat. Methods* 20, 205–213. <https://doi.org/10.1038/s41592-022-01685-y>.
- Huelsenbeck, J.P., Ronquist, F., 2001. MRBAYES: Bayesian inference of phylogenetic trees. *Bioinformatics* 17, 754–755. <https://doi.org/10.1093/bioinformatics/17.8.754>.
- Ito, A., et al., 1985. Effects of synthetic model peptides resembling the extension peptides of mitochondrial enzyme precursors on import of the precursors into mitochondria. *J. Biochem.* 98, 1571–1582. <https://doi.org/10.1093/oxfordjournals.jbchem.a135426>.
- Jia, S., Wan, P.J., Zhou, L.T., Mu, L.L., Li, G.Q., 2013. Knockdown of a putative Halloween gene Shade reveals its role in ecdysteroidogenesis in the small brown planthopper *Laodelphax striatellus*. *Gene* 531, 168–174. <https://doi.org/10.1016/j.gene.2013.09.034>.
- Jumper, J., et al., 2021. Highly accurate protein structure prediction with AlphaFold. *Nature* 596, 583–589. <https://doi.org/10.1038/s41586-021-03819-2>.
- Kalinina, O.V., Mironov, A.A., Gelfand, M.S., Rakhmaninova, A.B., 2004. Automated selection of positions determining functional specificity of proteins by comparative analysis of orthologous groups in protein families. *Protein Sci.* 13, 443–456. <https://doi.org/10.1110/ps.03191704>.
- Kumar, S., Stecher, G., Li, M., Nknyaz, C., Tamura, K., 2018. MEGA X: Molecular evolutionary genetics analysis across computing platforms. *Mol. Biol. Evol.* 35, 1547–1549. <https://doi.org/10.1093/molbev/msy096>.
- Laskowski, R.A., Rullmann, J.A., MacArthur, M.W., Kaptein, R., Thornton, J.M., 1996. AQUA and PROCHECK-NMR: programs for checking the quality of protein structures solved by NMR. *J. Biomol. NMR* 8, 477–486. <https://doi.org/10.1007/BF00228148>.
- Le, S.Q., Gascuel, O., 2008. An improved general amino acid replacement matrix. *Mol. Biol. Evol.* 25, 1307–1320. <https://doi.org/10.1093/molbev/msn067>.
- Li, M., Feng, X., Reid, W.R., Tang, F., Liu, N., 2023. Multiple-P450 gene Co-Up-Regulation in the development of permethrin resistance in the house fly, *Musca domestica*. *Int. J. Mol. Sci.* 24. <https://doi.org/10.3390/ijms24043170>.
- Li, W., et al., 2024. Comprehensive analysis of the overexpressed cytochrome P450-based insecticide resistance mechanism in *Spodoptera litura*. *J. Hazard Mater.* 461, 132605. <https://doi.org/10.1016/j.jhazmat.2023.132605>.
- Manjon, C., et al., 2018. Unravelling the molecular determinants of bee sensitivity to neonicotinoid insecticides. *Curr. Biol.* 28, 1137–1143. <https://doi.org/10.1016/j.cub.2018.02.045> e1135.
- Markstein, M., Pitsouli, C., Villalta, C., Celniker, S.E., Perrimon, N., 2008. Exploiting position effects and the gypsy retrovirus insulator to engineer precisely expressed transgenes. *Nat. Genet.* 40, 476–483. <https://doi.org/10.1038/ng.101>.
- Mazin, A.V., Mazina, O.M., Bugreev, D.V., Rossi, M.J., 2010. Rad54, the motor of homologous recombination. *DNA Repair* 9, 286–302. <https://doi.org/10.1016/j.dnarep.2009.12.006>.
- McIntosh, J.A., Heel, T., Buller, A.R., Chio, L., Arnold, F.H., 2015. Structural adaptability facilitates histidine heme ligation in a cytochrome P450. *J. Am. Chem. Soc.* 137, 13861–13865. <https://doi.org/10.1021/jacs.5b07107>.
- Mirdita, M., Steinegger, M., Söding, J., 2019. MMseqs2 desktop and local web server app for fast, interactive sequence searches. *Bioinformatics* 35, 2856–2858. <https://doi.org/10.1093/bioinformatics/bty1057>.
- Mirdita, M., et al., 2022. ColabFold: making protein folding accessible to all. *Nat. Methods* 19, 679–682. <https://doi.org/10.1038/s41592-022-01488-1>.
- Munro, A.W., McLean, K.J., Grant, J.L., Makris, T.M., 2018. Structure and function of the cytochrome P450 peroxxygenase enzymes. *Biochem. Soc. Trans.* 46, 183–196. <https://doi.org/10.1042/BST20170218>.
- Nauen, R., Slater, R., Sparks, T.C., Elbert, A., Mccaffery, A., 2019. *Modern Crop Protection Compounds* 995–1012.
- Nauen, R., Bass, C., Feyereisen, R., Vontas, J., 2022. The role of cytochrome P450s in insect toxicology and resistance. *Annu. Rev. Entomol.* 67, 105–124. <https://doi.org/10.1146/annurev-ento-070621-061328>.
- Nelson, D.R., et al., 1993. The P450 superfamily: update on new sequences, gene mapping, accession numbers, early trivial names of enzymes, and nomenclature. *DNA Cell Biol.* 12, 1–51. <https://doi.org/10.1089/dna.1993.12.1>.
- Nelson, D.R., et al., 1996. P450 superfamily: update on new sequences, gene mapping, accession numbers and nomenclature. *Pharmacogenetics* 6, 1–42. <https://doi.org/10.1097/00008571-199602000-00002>.
- Pan, X., et al., 2023. Identification and functional study of detoxification-related genes in response to tolfenpyrad stress in *Glyphodes pyloalis* Walker (Lepidoptera: Pyralidae). *Pestic. Biochem. Physiol.* 194, 105503. <https://doi.org/10.1016/j.pestbp.2023.105503>.
- Petryk, A., et al., 2003. Shade is the *Drosophila* P450 enzyme that mediates the hydroxylation of ecdysone to the steroid insect molting hormone 20-hydroxyecdysone. *Proc Natl Acad Sci U S A* 100, 13773–13778. <https://doi.org/10.1073/pnas.2336088100>.
- Pettersen, E.F., et al., 2004. UCSF Chimera—a visualization system for exploratory research and analysis. *J. Comput. Chem.* 25, 1605–1612. <https://doi.org/10.1002/jcc.20084>.
- Pfaffl, M.W., 2001. A new mathematical model for relative quantification in real-time RT-PCR. *Nucleic Acids Res.* 29, e45. <https://doi.org/10.1093/nar/29.9.e45>.
- Ratra, G.S., Casida, J.E., 2001. GABA receptor subunit composition relative to insecticide potency and selectivity. *Toxicol. Lett.* 122, 215–222. [https://doi.org/10.1016/S0378-4274\(01\)00366-6](https://doi.org/10.1016/S0378-4274(01)00366-6).
- Ritz, C., Baty, F., Streibig, J.C., Gerhard, D., 2015. Dose-response analysis using R. *PLoS One* 10, e0146021. <https://doi.org/10.1371/journal.pone.0146021>.
- Sangar, M.C., Bansal, S., Avadhani, N.G., 2010. Bimodal targeting of microsomal cytochrome P450s to mitochondria: implications in drug metabolism and toxicity. *Expet Opin. Drug Metabol. Toxicol.* 6, 1231–1251. <https://doi.org/10.1517/17425255.2010.503955>.
- Shi, Y., et al., 2022. Involvement of CYP2 and mitochondrial clan P450s of *Helicoverpa armigera* in xenobiotic metabolism. *Insect Biochem. Mol. Biol.* 140, 103696. <https://doi.org/10.1016/j.ibmb.2021.103696>.
- Stourac, J., et al., 2019. Caver Web 1.0: identification of tunnels and channels in proteins and analysis of ligand transport. *Nucleic Acids Res.* 47, W414–W422. <https://doi.org/10.1093/nar/gkz378>.
- Trott, O., Olson, A.J., 2010. AutoDock Vina: improving the speed and accuracy of docking with a new scoring function, efficient optimization, and multithreading. *J. Comput. Chem.* 31, 455–461. <https://doi.org/10.1002/jcc.21334>.
- Vatsis, K.P., Peng, H.-M., Coon, M.J., 2002. Replacement of active-site cysteine-436 by serine converts cytochrome P450 2B4 into an NADPH oxidase with negligible monooxygenase activity. *J. Inorg. Biochem.* 91, 542–553. [https://doi.org/10.1016/S0162-0134\(02\)00438-5](https://doi.org/10.1016/S0162-0134(02)00438-5).
- Wang, A., et al., 2023. A microRNA, PC-5p-30.205949, regulates triflumezopyrim susceptibility in *Laodelphax striatellus* (Fallén) by targeting CYP419A1 and ABCG23. *Pestic. Biochem. Physiol.* 192, 105413. <https://doi.org/10.1016/j.pestbp.2023.105413>.
- Warren, J.T., et al., 2002. Molecular and biochemical characterization of two P450 enzymes in the ecdysteroidogenic pathway of *Drosophila melanogaster*. *Proc Natl Acad Sci U S A* 99, 11043–11048. <https://doi.org/10.1073/pnas.162375799>.
- Wu, S.F., et al., 2018. The evolution of insecticide resistance in the brown planthopper (*Nilaparvata lugens* Stal) of China in the period 2012–2016. *Sci. Rep.* 8, 4586. <https://doi.org/10.1038/s41598-018-22906-5>.
- Xu, L., et al., 2020. Multiple down-regulated cytochrome P450 monooxygenase genes contributed to synergistic interaction between chlorpyrifos and imidacloprid against *Nilaparvata lugens*. *J. Asia Pac. Entomol.* 23, 44–50. <https://doi.org/10.1016/j.aspen.2019.10.017>.
- Yang, T., et al., 2021. Multiple cytochrome P450 genes: conferring high levels of permethrin resistance in mosquitoes, *Culex quinquefasciatus*. *Sci. Rep.* 11, 9041. <https://doi.org/10.1038/s41598-021-88121-x>.
- Ye, Y.X., et al., 2021. Chromosome-level assembly of the brown planthopper genome with a characterized Y chromosome. *Mol Ecol Resour* 21, 1287–1298. <https://doi.org/10.1111/1755-0998.13328>.
- Zhang, Y., et al., 2016. Synergistic and compensatory effects of two point mutations conferring target-site resistance to fipronil in the insect GABA receptor RDL. *Sci. Rep.* 6, 32335. <https://doi.org/10.1038/srep32335>.
- Zhang, W., et al., 2019. The roles of four novel P450 genes in pesticides resistance in *Apis cerana cerana fabricius*: expression levels and detoxification efficiency. *Front. Genet.* 10, 1000. <https://doi.org/10.3389/fgene.2019.01000>.
- Zhang, Y.C., et al., 2023. CRISPR/Cas9-mediated knockout of NICYP6CS1 gene reveals its role in detoxification of insecticides in *Nilaparvata lugens* (Hemiptera: Delphacidae). *Pest Manag. Sci.* 79, 2239–2246. <https://doi.org/10.1002/ps.7404>.
- Zimmer, C.T., et al., 2018. Neofunctionalization of duplicated P450 genes drives the evolution of insecticide resistance in the Brown planthopper. *Curr. Biol.* 28, 268–274. <https://doi.org/10.1016/j.cub.2017.11.060> e265.